Monte Carlo Simultaneous Localization of Multiple Unknown Transient Radio Sources Using a Mobile Robot with a Directional Antenna
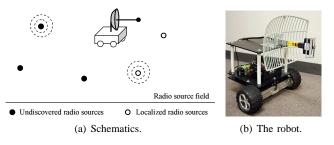
Dezhen Song, Chang-Young Kim, and Jingang Yi

Abstract— We report our system and algorithm developments that enable a single mobile robot equipped with a directional antenna to simultaneously localize multiple unknown transient radio sources. Due to signal source anonymity, short transmission durations, and dynamic transmission patterns, the robot cannot treat the radio sources as continuous radio beacons. To deal with challenging localization problem, we model the radio source behaviors using a novel spatiotemporal probability occupancy grid (SPOG) that captures transient characteristics of radio transmissions and tracks the spatiotemporal posterior probability distribution of the radio transmissions. As a Monte Carlo method, we propose a ridge walking motion planning algorithm that enables the robot to efficiently traverse the high probability regions to accelerate the convergence of the posterior probability distribution. We have implemented the algorithms and extensively tested them in comparison to a random walk and a fixed-route patrol mechanism. Our algorithms have shown consistently superior performance over their competitors.

Fig. 1. Schematics of deploying a single mobile robot to localize unknown transient radio sources. The radio sources with dashed circles indicate that they are sending radio signals.

I. INTRODUCTION

We report our system and algorithm developments that enable a single mobile robot equipped with a directional antenna to simultaneously localize multiple unknown transient radio sources. We intend to provide a countermeasure for the potential misuse of the fast-developing sensor network technology. A sensor network is usually composed of a large number of miniature wireless sensor nodes with self-configurable *ad hoc* networking capabilities. It may be used as a new espionage tool that threatens our security and privacy. This paper reports the first step of the study where we assume that there is only one robot available as illustrated in Figure 1. Since the robot is equipped with a directional antenna and on-board positional sensors, the robot can detect radio signal strengths (RSS) as it travels in the field of radio sources. When the radio sources and communication protocols are unknown, the robot cannot treat the radio sources as continuous radio beacons. More specifically,

- The number of radio sources is unknown.
- The periods of radio transmission are short.
- The signal source cannot be identified.
- Radio sources may not be active at all times and awaken intermittently.

D. Song and C. Kim are with CS Department, Texas A&M University, College Station, TX 77843, USA, (email: dzsong@cs.tamu.edu and kcyoung@cs.tamu.edu)

J. Yi is with MAE Department, Rutgers University, Piscataway, NJ 08854 USA, (email: jgyi@rutgers.edu)

To deal with this challenging localization problem, we model the radio source behaviors using a novel spatiotemporal probability occupancy grid (SPOG) that captures transient characteristics of radio transmissions and tracks their posterior probability distributions. We then propose an SPOG update algorithm that incrementally updates the SPOG as radio transmissions are intercepted. We also propose a Monte Carlo ridge walking motion planning algorithm that enables the robot to efficiently traverse high probability regions to accelerate the convergence of the posterior probability distributions of radio sources. We have implemented the algorithms and extensively tested them in comparison to a random walk and a fixed-route patrol mechanism. In experiments, our algorithms have shown consistently superior performance over its the two heuristics.

II. RELATED WORK

Localization of unknown transient radio sources relates to a variety of research fields including radio frequency-based localization, Simultaneous Localization and Mapping (SLAM), and occupancy grid methods.

The recent development of radio frequency-based localization can be viewed as the localization of "friendly" radio sources because researchers either assume that an individual radio source that continuously transmits radio signals (similar to a lighthouse) [1]–[5] or assume that the robot/receiver is a part of the network which understands the detailed packet information [6]–[12]. However, such information is not always available in an unknown network. In a recent work [2], Letchner et al. use a network of wireless access points to localize a mobile unit. This can be viewed as a dual version of our problem. They use multiple static listeners to localize a mobile transmitter, while we try to localize multiple static transmitters using a mobile listener. As another closely related work [9], Sichitiu and Ramadurai

try to localize sensor network nodes with a mobile beacon. Again, the mobile beacon and the sensor network nodes share the network information.

In robotics research, SLAM is defined as the process of mapping the environment and localizing robot position at the same time [13]–[17]. Although both SLAM and our approach are Bayesian approaches, SLAM assumes that the environment is static or close to static. Directly applying SLAM methods to our problem is not appropriate because networked radio sources create a highly dynamic environment where the signal transmission patterns change very quickly. Although recent advance in SLAM allows tracking of moving objects [18] while perform SLAM task, the environment largely remains static.

Since Elfes and Moravec [19], [20] introduce occupancy grid maps as a probabilistic sensor model, the occupancy grid has been proved to be an elegant representation of the sensor coverage for mobile robot applications such as localization and mapping [21]. Thrun and his colleagues [22], [23] further improve occupancy grid maps to incorporate multi-sensor fusion, an inverse sensor model, and a forward sensor model. Occupancy grid-based methods have recently been adapted to a variety of applications including gas/odor source localization [24]. The existing occupancy grid-based methods focus on using the spatial probabilistic representation to describe sensing uncertainty and are not capable of dealing with time-variant environments. In this work, we extend the occupancy grid methods into the temporal dimension to deal with the dynamic characteristics of the transient radio transmissions.
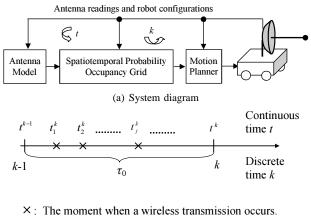
In our previous work, we use a single mobile robot equipped with a Log-Periodic Dipole Array antenna to localized unknown networked sensor nodes [25]. Using a particle filter approach, we assume that the carrier sensing multiple access (CSMA)-based protocol is used among the networked radio sources. In this paper, we relax the assumption and develop a protocol-independent localization scheme. We also notice the scalability issue of the particle filter method in the previous work and hence develop the SPOG to address the new localization problem.

III. SYSTEM DESIGN

Fig. 2(a) illustrates the hybrid system architecture. From the robot perspective, the input is the RSS readings from the directional antenna with the corresponding robot positions and antenna orientations. The output of the system is the planned trajectory for the robot to execute in the following period. The entire system is built around the SPOG, which tracks each cell's probability of containing a radio source and its transmission rate.

On the one hand, the system updates the SPOG whenever a radio transmission is detected by the antenna. The antenna model outputs the posterior probability distribution of the signal source as the inputs to the SPOG. This update process is described by a continuous time system. As a convention in this paper, we use t to denote the continuous time.

On the other hand, the robot plans its motion periodically. We define the period length as τ_0, which is carefully chosen

(a) System diagram

(b) System timing

$\times$: The moment when a wireless transmission occurs.

Fig. 2. An illustration of system diagram and timing.

to ensure the robot has enough time to execute the planned trajectory. At the beginning of each period, the robot plans its trajectory based on the current SPOG. This decision-making process is a discrete time system. We define $k \in \mathbb{N}$ as the discrete time index variable.

Fig. 2(b) illustrates the relationship between the continuous time system and the discrete time system. Let $t^k \in \mathbb{R}$ be the exact continuous time at the moment of the discrete time k. We define the k-th period as the time interval between t^{k-1} and t^k. Hence $t^k - t^{k-1} = \tau_0$ for $k > 1$. We also define $t_j^k \in \mathbb{R}$ as the exact continuous time when the j-th radio transmission occurs in the k-th period: $t^{k-1} \leq t_j^k < t^k$. The index variable j is set to zero at the beginning of each period.

IV. PROBLEM DEFINITION

A. Problem Setup

To formulate the localization problem, we make the following assumptions to setup the problem scenario,
1) Both the robot and radio sources are located in a free 2D Euclidean space.
2) The network traffic is light and each transmission is short. This is the typical characteristic of a low power sensor network.
3) The directional antenna on the robot has high sensitivity and can listen to all traffic. The robot can carry a large and highly sensitive antenna/amplifier.
4) The radio sources are static nodes.
5) Each radio transmission is transmitted at the same power level. This assumption can be relaxed if the robot is equipped with an orthogonal antenna pair, which can provide directional information regardless of the transmission power.
6) The radiation pattern of the radio sources is circular because most miniature wireless sensors are equipped with omni-directional antennas.

Due to the transient transmission and the fact that the robot cannot associate a signal with its source, the robot cannot simply triangulate the signal source. Since only one robot

is considered, the single perspective makes it more difficult than cases with multiple robots or receivers.

B. Spatiotemporal Probability Occupancy Grid

We introduce SPOG to track the posterior spatiotemporal distributions of radio sources. To define the SPOG, we partition the entire field into equally-sized square cells using a grid. Let us define cell index set $I := \{1, ..., n\}$, where n is the total number of cells. Define $i \in I$ as a cell index variable. The size of each cell is determined by the RSS resolution of the antenna. Inside each cell, we approximate radio source locations using cell center locations. Define C_i as the event that cell i contains at least one radio source and $P(C_i)$ as the probability that event C_i occurs. Hence $\sum_{i \in I} P(C_i)$ equals the number of cells that contain radio sources if $P(C_i)$ converges to a correct value in the Monte Carlo localization.

At time t_j^k, a transmission occurs. We define C_i^1 as the event that cell i is the active radio source at time t_j^k. Define C_i^0 as the event that cell i is inactive at time t_j^k. Hence

$$P(C_i^0) + P(C_i^1) = 1 \text{ and } \sum_{i \in I} P(C_i^1) = 1 \qquad (1)$$

because there is only one active transmission when the transmission is detected. We ignore the collision case because we take an RSS measurement as soon as the transmission is initiated. The probability of two or more transmissions that are initiated at the exact same moment is negligible in a light traffic network. C_i^1 is determined by the relative radio transmission rate and is the temporal part of the SPOG. Unlike a regular occupancy grid, the SPOG is unique because each cell is described by two types of correlated random events: the spatial event C_i and the temporal events C_i^0 and C_i^1.

C. Problem Formulation

Fig. 2(a) suggests that the overall localization problem can be divided into two sub problems: a sensing problem and a motion planning problem. Let random variable $Z_j^k \in [1, 255] \cap \mathbb{N}$ be the corresponding RSS reading at time t_j^k. Note that the RSS readings are from a receiver with a resolution of eight bits. Define $\mathbf{Z}(Z_j^k)$ as the set of all RSS values sensed from the beginning of the localization process to the moment when Z_j^k is sensed. We also define set $\mathbf{Z}^-(Z_j^k) := \mathbf{Z}(Z_j^k) - \{Z_j^k\}$, which is the set of all RSS readings from the beginning of the localization process to the moment right before Z_j^k is sensed. Define $P(C_i|\mathbf{Z}(Z_j^k))$ as the conditional probability that cell i contains at least one radio source given the RSS set $\mathbf{Z}(Z_j^k)$. Following the same convention, we define the conditional probabilities $P(C_i|\mathbf{Z}^-(Z_j^k))$, $P(C_i^1|\mathbf{Z}(Z_j^k))$, and $P(C_i^1|\mathbf{Z}^-(Z_j^k))$. The sensing problem updates the SPOG when a new transmission is detected,

Problem 1 (Sensing Problem): Given the current sensed RSS Z_j^k, previous RSS set $\mathbf{Z}^-(Z_j^k)$, $P(C_i|\mathbf{Z}^-(Z_j^k))$, $P(C_i^1|\mathbf{Z}^-(Z_j^k))$, and the corresponding robot configurations, compute $P(C_i|\mathbf{Z}(Z_j^k))$ and $P(C_i^1|\mathbf{Z}(Z_j^k))$ for each cell i.

At the beginning of each period k, we plan the robot trajectory for the period. Let us define the robot position and orientation as $\mathbf{r}(t) = [x(t), y(t), \theta(t)]^T \in \mathbb{R}^2 \times S$, where $S = (-\pi, \pi]$ is the orientation angle set. Since the antenna is fixed on the robot and points to the robot forwarding direction, $\theta(t)$ is also the antenna orientation. Define $j_{\max}$ as the index for the last transmission sensed in period k. Therefore, we can define the Monte Carlo motion planning problem for time k (or t^k) as,

Problem 2 (Radio Source Localization Motion Planning): Given the current SPOG, which are sets $\{P(C_i|\mathbf{Z}(Z_{j_{\max}}^k))|i \in I\}$ and $\{P(C_i^1|\mathbf{Z}(Z_{j_{\max}}^k))|i \in I\}$, plan robot trajectory $\{\mathbf{r}(t)|t^k \leq t < t^{k+1}\}$ that enables the robot to quickly localize radio sources.

V. Modeling

A. Sensing Problem

We address the sensing problem first. The sensing problem actually has two components: an antenna model and an SPOG update process.
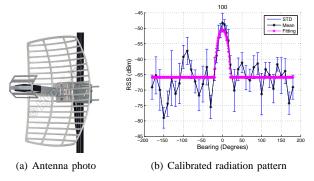

(a) Antenna photo   (b) Calibrated radiation pattern

Fig. 3.   HyperGain HG2415G parabolic directional antenna properties.

1) Antenna Model: The antenna model describes the property of the directional antenna. As illustrated in Figure 3, we use an HyperGain HG2415G parabolic antenna in our system. Bearing and distance are the two most important variables in an antenna model [26]. Let $(x_j^k, y_j^k, \theta_j^k)$ be the robot configuration when the j-th radio transmission in the k-th period is sensed. Let (x_i, y_i) be the cell center location. Define d_{ij}^k as the distance from robot to the center of the cell,

$$d_{ij}^k = \sqrt{(x_j^k - x_i)^2 + (y_j^k - y_i)^2}. \qquad (2)$$

Let ϕ_{ij}^k be the bearing of the cell with respect to the robot,

$$\phi_{ij}^k = \text{atan2}(x_j^k - x_i, y_j^k - y_i) - \theta_j^k. \qquad (3)$$

Assume the active radio source is located in cell i, the expected RSS s_i of the directional antenna is given as,

$$s_i = C \cdot (d_{ij}^k)^{-\beta} s(\phi_{ij}^k), \qquad (4)$$

where C is a constant depending on radio transmission power and $(d_{ij}^k)^{-\beta}$ is the signal decay function. The directivity of the antenna is captured by the term $s(\phi_{ij}^k)$, which describes the radiation pattern of the antenna. We set $C = 1.77$ and the decay factor $\beta = 2.65$ for our antenna, which are obtained

from our antenna calibration process. Our β values conforms to the widely-accepted notion that the decay factor is between 2 and 4 [27].

Since our receiver uses dBm as RSS unit, we have to take a $10 \log 10$ with respect to (4),

$$z_0 = 10\big(\log_{10} C - \beta \log_{10} d_{ij}^k + \log_{10} s(\phi_{ij}^k)\big), \quad (5)$$

where z_0 is the expected RSS in units of dBm. From the antenna theory and the results from antenna calibration, we perform curve-fitting to obtain the radiation pattern function as illustrated Fig. 3(b),

$$s(\phi_{ij}^k) = \begin{cases} \cos^2\left(4\phi_{ij}^k\right) & \text{if } -20° \le \phi_{ij}^k \le 20°, \\ \cos^2\left(80°\right) & \text{otherwise.} \end{cases} \quad (6)$$

Note that the peak at the zero bearing in Fig. 3(b) is about 15 dBm higher than the average of non-peak regions. Although the data in Fig. 3(b) is obtained from the antenna calibration, the result conforms to antenna specifications well.

Eqs. (5) and (6) describe the expected RSS given that the radio transmission is from cell i. However, the sensed RSS is not a constant but a random variable due to the uncertainties in radio transmissions. Define Z_j^k as the sensed RSS. Therefore, the mean value of Z_j^k is z_0. From the antenna calibration, we know that Z_j^k conforms to the truncated normal distribution with a density function of

$$g(z) = \frac{\frac{1}{\sigma} f\left(\frac{z-z_0}{\sigma}\right)}{F\left(\frac{z_{\max}-z_0}{\sigma}\right) - F\left(\frac{z_{\min}-z_0}{\sigma}\right)}, \quad (7)$$

where the value of σ is 3.3 that is obtained from the antenna calibration, z is the sensed RSS value, $f(\cdot)$ is the probability density function (PDF) of a normal distribution with zero mean and unit variance, $F(\cdot)$ is the cumulative distribution function (CDF) of $f(\cdot)$, and $z_{\min}$ and $z_{\max}$ are the minimum and the maximum RSS that the antenna can sense, respectively. Let

$$G(z) = \int_{z_{\min}}^z g(z)dz \quad (8)$$

be the CDF of the truncated normal distribution.

Define $P(Z_j^k = z|C_i^1)$ as the conditional probability that the sensed signal strength is an integer z given cell i contains at least an active radio source. $P(Z_j^k = z|C_i^1)$ actually is the overall antenna model. Since Z_j^k can only take integer values, we have

$$P(Z_j^k = z|C_i^1) = G(z + 0.5) - G(z - 0.5). \quad (9)$$

2) Updating Probability Occupancy Grid: When a radio transmission with an RSS level of z is sensed, we are interested in $P(C_i|Z_j^k = z)$, which is the conditional probability that cell i contains at least one radio source given the sensed RSS is z. According to (1), we have

$$P(C_i|Z_j^k = z) = P(C_i, C_i^1|Z_j^k = z) + P(C_i, C_i^0|Z_j^k = z).$$

Since event C_i^1 implies event C_i, the joint event (C_i, C_i^1) is the same as C_i^1. Hence,

$$P(C_i|Z_j^k = z) = P(C_i^1|Z_j^k = z) + P(C_i, C_i^0|Z_j^k = z). \quad (10)$$

According to Bayes' theorem,

$$P(C_i^1|Z_j^k = z) = \frac{P(Z_j^k = z|C_i^1)P(C_i^1)}{\sum_{i \in I} P(Z_j^k = z|C_i^1)P(C_i^1)}. \quad (11)$$
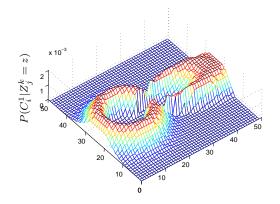

Fig. 4.   The distribution of $P(C_i^1|Z_j^k = z)$ over a 50×50 grid for the directional antenna given that $P(C_i^1)$ is the same across all cells.

Eq. (11) describes the posterior conditional distribution of the active radio source given the sensed signal strength is z. If we assume that the radio transmission is equally likely to be initiated by any cell in the grid, which means that $P(C_i^1)$ is the same across all cells, then the posterior condition distribution is very similar to the radiation pattern as illustrated in Fig. 4.

The second term $P(C_i, C_i^0|Z_j^k = z)$ in (10) is the joint conditional probability that there is at least one radio source in cell i and none of the radio sources in cell i transmits given the sensed RSS is z. Joint event (C_i, C_i^0) implies the following information:

- Since cell i is not transmitting, condition $Z_j^k = z$ cannot provide additional information for event C_i, which implies $P(C_i|Z_j^k = z) = P(C_i)$.
- There must be one active cell s, $s \in I$ and $s \ne i$.
- Joint conditional event $(C_i, C_i^0|Z_j^k = z)$ is equivalent to the union of the collection of events $\{(C_i, C_s^1|Z_j^k = z), s \ne i, s \in I\}$ because of no collision.
- Events C_i and C_s^1 are independent.

Therefore, we can obtain,

$$P(C_i, C_i^0|Z_j^k = z) = P(C_i) \sum_{s \ne i, s \in I} P(C_s^1|Z_j^k = z) \quad (12)$$

Note that $P(C_s^1|Z_j^k = z)$ can be computed using (11). Plugging (11) and (12) into (10), we get,

$$P(C_i|Z_j^k = z) =$$
$$\frac{\left(\begin{array}{c} P(Z_j^k = z|C_i^1)P(C_i^1) + \\ P(C_i) \sum_{s \ne i, s \in I} P(Z_j^k = z|C_s^1)P(C_s^1) \end{array}\right)}{\sum_{i \in I} P(Z_j^k = z|C_i^1)P(C_i^1)} \quad (13)$$

Unfortunately, (11) and (13) cannot be directly used in the system because $P(C_i)$ and $P(C_i^1)$ are not available. We have to rely on the conditional versions of $P(C_i)$ and $P(C_i^1)$ that build on the observation $\mathbf{Z}^-(Z_j^k)$. We can derive the

following from (11) by adding $\mathbf{Z}^-(Z_j^k)$ as the condition,

$$P(C_i^1|\{Z_j^k = z\} \cup \mathbf{Z}^-(Z_j^k)) = \frac{P(Z_j^k = z|C_i^1, \mathbf{Z}^-(Z_j^k))P(C_i^1|\mathbf{Z}^-(Z_j^k))}{\sum_{i \in I} P(Z_j^k = z|C_i^1, \mathbf{Z}^-(Z_j^k))P(C_i^1|\mathbf{Z}^-(Z_j^k))}. \quad (14)$$

Since the conditional event $Z_j^k = z$ is independent of the previous RSS values $\mathbf{Z}^-(Z_j^k)$ given C_i^1, we know $P(Z_j^k = z|C_i^1, \mathbf{Z}^-(Z_j^k)) = P(Z_j^k = z|C_i^1)$. According to the definition, $\{Z_j^k = z\} \cup \mathbf{Z}^-(Z_j^k) = \mathbf{Z}(Z_j^k)$. Eq. (14) can be rewritten as,

$$P(C_i^1|\mathbf{Z}(Z_j^k)) = \frac{P(Z_j^k = z|C_i^1)P(C_i^1|\mathbf{Z}^-(Z_j^k))}{\sum_{i \in I} P(Z_j^k = z|C_i^1)P(C_i^1|\mathbf{Z}^-(Z_j^k))}. \quad (15)$$

Similarly, from (13), we can derive the following,

$$P(C_i|\mathbf{Z}(Z_j^k)) = \frac{\left(\begin{array}{c} P(Z_j^k = z|C_i^1)P(C_i^1|\mathbf{Z}^-(Z_j^k)) + \\ P(C_i|\mathbf{Z}^-(Z_j^k)) \times \\ \sum_{s \neq i, s \in I} P(Z_j^k = z|C_s^1)P(C_s^1|\mathbf{Z}^-(Z_j^k)) \end{array} \right)}{\sum_{i \in I} P(Z_j^k = z|C_i^1)P(C_i^1|\mathbf{Z}^-(Z_j^k))} \quad (16)$$

Eqs. (15) and (16) provide a recursive formulation for updating SPOG when a new radio transmission is sensed.

If we have unlimited resources and place a robot in each cell, then $P(C_i|\mathbf{Z}(Z_j^k)) \to 1$ for cells that contains radio sources and $P(C_i|\mathbf{Z}(Z_j^k)) \to 0$ for other cells as $k \to \infty$. This can be formally proved by introducing radio transmission arrival process model. However, this clear binary distribution cannot be achieved due to limited robot perspectives. Since we threshold $P(C_i|\mathbf{Z}(Z_j^k))$ to determine if cell i contains at least a radio source, the convergence rate of the SPOG determines localization speed and accuracy. If we take a close look at (15) and (16), it is clear that the update of the SPOG largely depends the antenna model $P(Z_j^k = z|C_i^1)$, which actually is a function of robot configurations. Hence, the convergence of the SPOG and the corresponding convergence speed really depend on the robot motion planning.

B. Robot Motion Planner

The intuition is to accelerate the rate that $P(C_i|\mathbf{Z}(Z_j^k)) \to 1$ for cells that contains radio sources with high probabilities through effective robot motions. Take a close look at (16), the update process contains two parts:

$$P(C_i|\mathbf{Z}(Z_j^k)) = P(C_i^1|\mathbf{Z}(Z_j^k)) + P(C_i, C_i^0|\mathbf{Z}(Z_j^k)),$$

where

$$P(C_i, C_i^0|\mathbf{Z}(Z_j^k)) = \frac{P(C_i|\mathbf{Z}^-(Z_j^k)) \sum_{s \neq i, s \in I} P(Z_j^k = z|C_s^1)P(C_s^1|\mathbf{Z}^-(Z_j^k))}{\sum_{i \in I} P(Z_j^k = z|C_i^1)P(C_i^1|\mathbf{Z}^-(Z_j^k))}. \quad (17)$$

Since joint event (C_i, C_i^0) offers no more information regarding C_i, we ignore this part. Therefore, to increase the value of $P(C_i|\mathbf{Z}(Z_j^k))$, we want to increase $P(C_i^1|\mathbf{Z}(Z_j^k))$ as much as possible. According to (15), this means

$$\max \frac{P(Z_j^k = z|C_i^1)P(C_i^1|\mathbf{Z}^-(Z_j^k))}{\sum_{s \in I} P(Z_j^k = z|C_s^1)P(C_s^1|\mathbf{Z}^-(Z_j^k))}. \quad (18)$$

Since $P(C_i^1|\mathbf{Z}^-(Z_j^k))$s are constants at the time, the quantity above achieves its maximum when $P(Z_j^k = z|C_i^1)$ achieves its maximum by adjusting z value,

$$\max_z P(C_i^1|\mathbf{Z}^-(Z_j^k)). \quad (19)$$

We omit the process of deriving the optimal solution for (18) and (19) for brevity. Eq. (19) achieves its maximum when z is at its maximum. This means that the robot has to place its antenna's most sensitive region over the cell that has a high probability of containing radio sources.

Eqs. (5), (4), and (6) suggest that the most sensitive region is located at zero bearing angle and at the nearest distance. Combining this, it is clear that the principle of the motion planning is to place the robot into the cells with the high $P(C_i|\mathbf{Z}(Z_j^k))$ values and force the robot to face these cells as much as possible. This principle inspires us to develop a Ridge Walking Algorithm (RWA) for the robot motion planning.
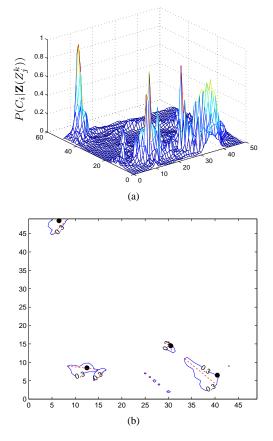

(a)

(b)

Fig. 5. (a) An example of $P(C_i|\mathbf{Z}(Z_j^k))$ distribution, (b) Radio source locations, a sample level set $L(0.3)$, and ridges over a 50×50 grid for the case. The radio source locations are shown in black dots. Level set is bounded inside the blue solid lines. The red dashed lines are the corresponding ridges for the level set components.

Fig. 5(a) illustrates an example of the distribution of

$P(C_i|\mathbf{Z}(Z_j^k))$ over a 50×50 grid. The actual radio source positions are shown as black dots in Fig. 5(b). $P(C_i|\mathbf{Z}(Z_j^k))$ value is much larger in the area adjacent to radio sources than that of other areas. To study the spatial distribution of $P(C_i|\mathbf{Z}(Z_j^k))$, we introduce level set $L(p)$, $p \in (0,1]$ as follows,

$$L(p) = \{i | P(C_i|\mathbf{Z}(Z_j^k)) \geq p, i \in I\}. \qquad (20)$$

Let us envision that a plane parallel to the ground plane intersects the mountain-like $P(C_i|\mathbf{Z}(Z_j^k))$ distribution at height p in Fig. 5(a). The intersection generates $L(p)$ which contains all cells with $P(C_i|\mathbf{Z}(Z_j^k))$ above the plane. Fig. 5(b) illustrates the level set $L(0.3)$ for the example in Fig. 5(a).

Fig. 5(b) also shows that $L(p)$ usually consists of several disconnected components. Define l_{max} as the total number of the disconnected components and L_l as the l-th component, $l = 1, ..., l_{max}$. Therefore, $L(p) = L_1 \cup L_2 \cup ... \cup L_{l_{max}}$, and $L_l \cap L_m = \emptyset$, where $m \neq l$ and $m = 1, 2, .., l_{max}$. For the l-th component, we define its ridge R_l as the line segment defined by points (x', y') and (x'', y'') on L_l,

$$R_l = \{(x,y) | x = (1-\alpha)x' + \alpha x'',$$
$$y = (1-\alpha)y' + \alpha y'', \alpha \in [0,1]\}, \qquad (21)$$

where points (x', y') and (x'', y'') are the two points on L_l such that the distance between (x', y') and (x'', y'') is the maximum.

If the robot walks on the ridge, the probability that the robot is close to a potential radio source is very high. Due to the walking direction, the antenna is always pointed along the ridge, which ensures the most sensitive reception region of the antenna to overlap with the l-th component. In the RWA algorithm, there are two types of robot motion: on-ridge movements and off-ridge movements. Since the on-ridge movement is the effective movement for the localization purpose, it is desirable for the robot to allocate its time to on-ridge movements as much as possible. The off-ridge movement refers to the travel in-between ridges for the robot. Since we have a fixed time period, we set the robot to travel at its fastest speed along the shortest path for off-ridge movements to save time for on-ridge movements.

Since each ridge is usually short, we can approximate each ridge as a vertex. We define edges as the line segments connecting different vertices on the 2D plane. With a vertex set V, an edge set E and a graph $G(V, E)$, to find the shortest path for the off-ridge movement is an instance of the traveling salesman problem (TSP) problem. Although the decision version of the planar TSP problem is NP-complete, we can use the 3-opt heuristics to solve it [28]. If a better approximation result is needed, we can use other approximation algorithms [29]. Those algorithms give us a close to the shortest off-ridge movement trajectory. Define v_{max} as the maximum velocity that the robot can travel. The time available for on-ridge movements t_{ON} is,

$$t_{ON} = \tau_0 - d_{OFF}/v_{max}, \qquad (22)$$

where d_{OFF} is the total length of off-ridge edges. We allocate t_{ON} to each ridge proportional to the probability that the corresponding component contains a radio source. For component l, we define the time the robot spend on the ridge R_l as τ_l. Therefore,

$$\tau_l = \frac{\sum_{i \in L_l} P(C_i|\mathbf{Z}(Z_j^k))}{\sum_{i \in L(p)} P(C_i|\mathbf{Z}(Z_j^k))} t_{ON}. \qquad (23)$$

With τ_l and the length of each ridge, it is trivial to find the robot velocity for the ridge.

VI. ALGORITHMS

To summarize our analysis, we present two algorithms including an SPOG update algorithm and the RWA. Corresponding to the sensing problem in Section IV-C, the SPOG update algorithm runs when a radio signal is detected. Define set $\mathbb{C}^*$ as the set of cells that contain radio sources with initial value $\mathbb{C}^* = \emptyset$. Define p_t as the probability threshold for finding the radio source. The robot reports the cells that satisfy $P(C_i|\mathbf{Z}(Z_j^k)) > p_t$ as the cells that contain at least one radio source. Recall that n is the total number

---

Algorithm 1: SPOG Update Algorithm

input : the received RF signal strength $Z_j^k = z$
output: $P(C_i|\mathbf{Z}(Z_j^k))$, $P(C_i^1|\mathbf{Z}(Z_j^k))$, $i \in I$, and $\mathbb{C}^*$
for $i \in I$ **do** $\qquad O(n)$
    Compute distance d_{ij}^k using (2); $\qquad O(1)$
    Compute bearing ϕ_{ij}^k using (3); $\qquad O(1)$
    Compute radiation pattern $s(\phi_{ij}^k)$ using (6); $\quad O(1)$
    Compute z_0 using (5); $\qquad O(1)$
    Compute $g(z)$ using (7); $\qquad O(1)$
    Compute $G(z)$ using (8); $\qquad O(1)$
    Compute $P(Z_j^k = z|C_i^1)$ using (9); $\qquad O(1)$
for $i \in I$ **do** $\qquad O(n)$
    Compute $P(C_i^1|\mathbf{Z}(Z_j^k))$ using (15); $\qquad O(n)$
    Compute $P(C_i|\mathbf{Z}(Z_j^k))$ using (16); $\qquad O(n)$
    if $P(C_i|\mathbf{Z}(Z_j^k)) > p_t$ **and** $i \notin \mathbb{C}^*$ **then**
        $\mathbb{C}^* = \mathbb{C}^* \cup \{i\}$; $\qquad O(1)$

---

of cells. It is clear that the SPOG update algorithm runs $O(n^2)$. The initial value settings are $P(C_i|\mathbf{Z}(Z_0^0)) = 0$ and $P(C_i^1|\mathbf{Z}(Z_0^0)) = 1/n$.

The RWA algorithm runs every τ_0 time. As illustrated in Algorithm 2, the robot performs random walking until set $L(p) \neq \emptyset$ at the initialization stage. Then the robot switches into the normal ridge walking mode. The robot stops when no additional radio source has been found in k_{max} consecutive periods where k_{max} is a preset iteration number. Algorithm 2 uses exhaustive search to find the exact TSP tour. The overall complexity is $O(n + (l_{max} - 1)!)$. Although the 3-opt heuristic can accelerate the computation of the TSP, it cannot change the worst case complexity.

VII. EXPERIMENTS

We have implemented the algorithms and the simulation platform using Microsoft Visual C++ .NET 2005 with OpenGL on a PC Desktop with an Intel 2.13GHz Core 2 Duo

Algorithm 2: Ridge Walking Algorithm

---

input : $P(C_i|\mathbf{Z}(Z_j^k))$, $P(C_i^1|\mathbf{Z}(Z_j^k))$, $i \in I$

output: Robot motion $\{\mathbf{r}(t)|t^k \le t < t^{k+1}\}$ and $\mathbb{C}^*$

Compute $L(p)$; $O(n)$

if $L(p) = \emptyset$ **then**

     $\{\mathbf{r}(t)|t^k \le t < t^{k+1}\}$ = random walk; $O(1)$

else

     Find all disconnected components in $L(p)$; $O(n)$

     Compute R_l for each L_l; $O(n)$

     Construct graph G and solve TSP; $O((l_{\max} - 1)!)$

     Compute d_{OFF}; $O(l_{\max})$

     Compute t_{ON} using (22); $O(1)$

     Compute τ_l for each ridge using (23); $O(1)$

     Output robot motion $\{\mathbf{r}(t)|t^k \le t < t^{k+1}\}$; $O(1)$

Fig. 6. RWA performance vs. τ_0.

Fig. 7. Convergence of $P(C_i|\mathbf{Z}(Z_j^k))$ at radio source locations for a six-radio source case.

CPU and 2GB RAM. The machine runs Microsoft Windows XP. The algorithms are tested in the simulation. The antenna on the robot is HyperGainT Model HG2415G which is a 2.4 GHz 15 dBi Reflector Grid Antenna. The radio sources are Zigbee nodes which are XBeeT with ZigBeeT/802.15.4 OEM radio frequency Modules by MaxStream, Inc. The antenna is calibrated first with the radio sources. The calibration is conducted at 328 configurations and 6560 readings have been collected. The calibrated antenna model is represented as the coefficients in (5) and σ in (7). We use the data from the real hardware to drive the simulation experiments below.

The grid is a square with 50×50 cells. Each grid cell has a size of 5.08×5.08 cm^2. Each radio source generates radio transmission signals according to an independently and identically distributed Poisson process with a rate of $\lambda = 0.012$ packets per second. The threshold $p_t = 0.8$ and the level set parameter $p = \frac{6}{n} \sum_i P(C_i|\mathbf{Z}(Z_j^k))$, where the constant 6 is determined by many experimental trials. During each trial of the simulation, we randomly generate radio source locations in the 50×50 grid.

The first experiment we conducted is to study how fast an RWA can localize all radio sources under different τ_0 settings. This determines how often we should run the RWA algorithm. Fig. 6 summarizes the test results. We change the radio source number from 2 to 10 during the simulation. Each point in Fig. 6 is an average of 10 trials. It is interesting that the RWA is at its best performance when $\tau_0 = 800$ seconds regardless of the radio source number. This means that the robot need to listen to each radio for an expected value of $800\lambda = 9.6$ times before repeating the algorithm.

Fig. 7 illustrates how $P(C_i|\mathbf{Z}(Z_j^k))$ converges at the radio source for a trial with six radio sources. The location of the six radio sources is shown in Fig. 5(b). It is clear that $P(C_i|\mathbf{Z}(Z_j^k))$ grows monotonically toward 1. This is what we expect to see: $P(C_i|\mathbf{Z}(Z_j^k)) \to 1$ for cells contains radio sources.

We also compare our algorithms to two intuitive heuristics, namely, a random walk and a fixed-route patrol. The random walk is chosen because it is considered as the most conservative approach. 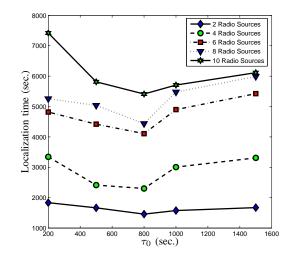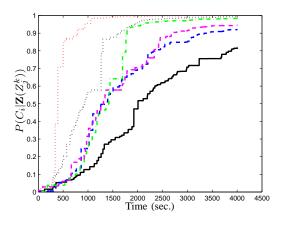Over a long run, a random walk can cover the entire field. Hence it does not have a blind spot. The fixed-route patrol traverses the field using a pre-defined route. It is considered as energy efficient but might not treat each cell equally due to the route selection. We increase the radio source number from 2 to 10 to observe the performance of each method. For each trial, we test all three methods. We repeat for 10 trials for each radio source number and compute the average time required for localizing all radio sources. Fig. 8 illustrates comparison results. It is clear that the RWA significantly outperforms the two heuristics. It is also surprising that the fixed route patrol is no much better than the random walk. However, the result can be explained that the robot motion for the two heuristics does not consider sensor location distribution and hence cannot achieve good performance.

VIII. CONCLUSIONS AND FUTURE WORK

We report our system and algorithm developments that enable a mobile robot equipped with a directional antenna to localize unknown transient radio sources. Employing a Monte Carlo approach, we modeled the radio transmission
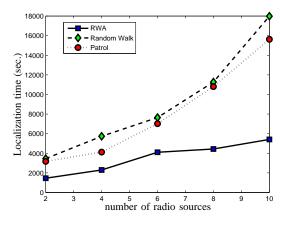
Fig. 8. Localization performance comparison among the RWA, the random walk, and the fixed-route patrol.

activities using an SPOG and proposed an SPOG update algorithm and an RWA algorithm for robot motion planning. For a n-cell grid, the SPOG update algorithm runs in $O(n^2)$ time and the RWA runs in $O(n+(l_{max}-1)!)$ time. We tested the algorithm using simulation with the data from the real hardware. In the experiment, we compared our algorithms with a random walk and a fixed-route patrol heuristics. Our algorithms showed a consistently superior performance over the two heuristics. We are currently testing our algorithm using physical experiments. Results will be reported in subsequent revisions. We are also interested in designing a multiple-robot localization scheme and will consider an approach to localize moving radio sources.

REFERENCES

[1] P. Bahl and V. N. Padmanabhan, "RADAR: An in-building RF-based user location and tracking system," in *INFOCOM'00*, 2000, pp. 775–784.

[2] J. Letchner, D. Fox, and A. LaMarce, "Large-scale localization from wireless signal strength," in *Proc. of the National Conference on Artificial Intelligence (AAAI-05)*, 2005.

[3] N. Malhotra, M. Krasniewski, C. Yang, S. Bagchi, and W. Chappell, "Location estimation in ad hoc networks with directional antennas," in *Proceedings of the 25th IEEE International Conference on Distributed Computing Systems (ICDCS'05)*. Washington, DC, USA: IEEE Computer Society, 2005, pp. 633–642.

[4] M. Youssef, A. Agrawala, and U. Shankar, "Wlan location determination via clustering and probability distributions," in *IEEE PerCom 2003*, 2003, p. 143.

[5] G. Mao, B. Fidan, and B. Anderson, "Wireless sensor network localization techniques," *Computer Networks*, vol. 51, no. 7, pp. 2529–2553, 2007.

[6] N. Bulusu, J. Heidemann, and D. Estrin, "Gps-less low cost outdoor localization for very small devices," *IEEE Personal Communications Magazine*, vol. 7, no. 5, pp. 28–34, October 2000.

[7] X. Ji and H. Zha, "Sensor positioning in wireless ad-hoc sensor networks using multidimensional scaling," in *INFOCOM*, 2004, pp. 2562–2661.

[8] K. Lorincz and M. Welsh, "Motetrack: A robust, decentralized approach to rf-based location tracking," in *Proceedings of the International Workshop on Location and Context-Awareness (LoCA 2005) at Pervasive 2005*, 2005, pp. 63–82.

[9] M. Sichitiu and V. Ramadurai, "Localization of wireless sensor networks with a mobile beacon," in *first IEEE International conference on Mobile Ad hoc and Sensor Systems*, 2004, pp. 174 – 183.

[10] N. Bulusu, V. Bychkovskiy, D. Estrin, and J. Heidemann, "Scalable, ad hoc deployable rf-based localization," in *Grace Hopper Celebration of Women in Computing Conference 2002, Vancouver, British Columbia, Canada.* University of California at Los Angeles, October 2002. [Online]. Available: http://www.cs.ucla.edu/ bulusu/papers/Bulusu02a.html

[11] D. Koutsonikolas, S. Das, and Y. Hu, "Path planning of mobile landmarks for localization in wireless sensor networks," *Computer Comunications*, vol. 30, pp. 2577–2592, 2007.

[12] T. Sit, Z. Liu, M. A. Jr., and W. Seah, "Multi-robot mobility enhanced hop-count based localization in ad hoc networks," *Robotics and Autonomos Systems*, vol. 55, pp. 244–252, 2007.

[13] S. Thrun, "Robotic mapping: A survey," in *Exploring Artificial Intelligence in the New Millenium*, G. Lakemeyer and B. Nebel, Eds. Morgan Kaufmann, 2002.

[14] M. W. M. G. Dissanayake, P. Newman, S. Clark, H. F. Durrant-Whyte, and M. Csorba, "A solution to the simultaneous localization and map building (slam) problem," *IEEE Transactions on Robotics and Automation*, vol. 17, no. 3, pp. 229–241, 2001.

[15] D. Hähnel, W. Burgard, D. Fox, K. Fishkin, and M. Philipose, "Mapping and localization with RFID technology," in *Proc. of the IEEE International Conference on Robotics and Automation (ICRA)*, 2004, pp. 1015–1020.

[16] K. P. Murphy, "Bayesian map learning in dynamic environments," in *NIPS*, 1999, pp. 1015–1021.

[17] D. Fox, S. Thrun, F. Dellaert, and W. Burgard, "Particle filters for mobile robot localization," in *Sequential Monte Carlo Methods in Practice*, A. Doucet, N. de Freitas, and N. Gordon, Eds. New York: Springer Verlag, 2000.

[18] C. Wang, C. Thorpe, S. Thrun, M. Hebert, and H. Durrant-Whyte, "Simultaneous localization, mapping and moving object tracking," *The International Journal of Robotics Research*, vol. 26, no. 9, pp. 889–916, September 2007.

[19] A. Elfes, "Occupancy grids: A probabilistic framework for robot perception and navigation," Ph.D. dissertation, Department of Electrical and Computer Engineering, Carnegie Mellon University, 1989.

[20] Moravec and H.P., "Sensor fusion in certainty grids for mobile robots," *AI Magazine*, no. 9, pp. 61–74, 1988.

[21] S. Thrun, "Learning metric-topological maps for indoor mobile robot navigation," *Artificial Intelligence*, no. 99, pp. 21–71, 1998.

[22] S.Thrun, "Learning occupancy grid maps with forward sensor models," *Autonomous Robots*, no. 15, pp. 111–127, 2003.

[23] S. Thrun, W. Burgard, and D. Fox, *Probabilistic Robotics*. MIT Press, 2005.

[24] G. Ferri, M. Jakuba, E. Caselli, V. Mattoli, B. Mazzolai, D. Yoerger, and P. Dario, "Localizing multiple gas/odor sources in an indoor environment using bayesian occupancy grid mapping," in *International Conference on Intelligent Robots and Systems (IROS)*, Nov. 2007, pp. 566–571.

[25] D. Song, J. Yi, and Z. Goodwin, "Localization of unknown networked radio sources using a mobile robot with a directional antenna," in *the American Control Conference (ACC), New York City, USA, July*, 2007, pp. 5952–5957.

[26] W. L. Stutzman and G. A. Thiele, *Antenna Theory and Design*. John Wiley & Sons, Inc., 2003.

[27] R. S. Elliott, *Antenna Theory and Design*. The IEEE Press, 2003.

[28] S. Lin, "Computer solutions of the traveling-salesman problem," *Bell System Technology Journal*, vol. 44, pp. 2245–2269, 1965.

[29] S. Arora, "Polynomial time approximation schemes for euclidean tsp and other geometric problems," *Journal of the ACM*, vol. 45, no. 5, pp. 753–782, September 1998.